

Article

Global Feedback Control for Coordinated Linear Switched Reluctance Machines Network with Full-State Observation and Internal Model Compensation

Bo Zhang ^{1,2} , Jianping Yuan ^{2,*}, J. F. Pan ^{1,*} , Xiaoyu Wu ¹, Jianjun Luo ² and Li Qiu ¹

¹ College of Mechatronics and Control Engineering, Shenzhen University, Shenzhen 518060, China; zhangbo@szu.edu.cn (B.Z.); wuxy@szu.edu.cn (X.W.); qiuli@szu.edu.cn (L.Q.)

² Laboratory of Advanced Unmanned Systems Technology, Research Institute of Northwestern Polytechnical University in Shenzhen, Shenzhen 518060, China; jjluo@nwpu.edu.cn

* Correspondence: jianpingyuan@yeah.net (J.Y.); pjf@szu.edu.cn (J.F.P.); Tel.: +86-755-2653-5382 (J.F.P.)

Received: 12 October 2017; Accepted: 27 November 2017; Published: 2 December 2017

Abstract: This paper discusses the tracking coordination of a linear switched reluctance machine (LSRM) network based on a global feedback control strategy with a full-state observation framework. The observer is allocated on the follower instead of the leader to form a leader–follower–observer network, by utilizing the leader as the global feedback tracking controller and the observer as the observation of the full states. The internal model compensator (IMC) is applied to the leader for the improvement of the network performance. The full-state information of the LSRM network is reconfigured by the output of the LSRM where the observer is located to provide necessary feedback information to the leader. Then, the controllability and observability of the leader–follower–observer network with the IMC are inspected, serving as a basis for the design of the global controller with the IMC and full-state observer. Experimentation verifies the effectiveness of the proposed network control scheme and the results demonstrate that both the absolute and the relative accuracy can be simultaneously improved, compared to the LSRM network with only the consensus algorithm and no global feedback mechanism.

Keywords: leader–follower–observer network; network controllability; IMC; linear machine

1. Introduction

Linear motions can be found throughout industry, and linear motions realized by direct-drive, linear machines have many advantages, such as fast response, high precision, and the annihilation of accumulated errors [1]. For multi-directional linear motions, several direct-drive, linear machines can be arranged to work together to accomplish one ultimate task. For example, as shown in Figure 1, in the frame assembly process for automobiles, a linear machine is responsible for transporting the frame, while two or more linear machines can be applied to perform operations such as drilling, welding or screwing. The entire processing procedure is often realized in a sequenced manner, i.e., each processing unit cannot execute until its former actions are finished, and each process should also follow its required individual reference signal precisely to guarantee a certain “absolute” tracking precision. Meanwhile, current action must become fully settled before any other process starts. If there occurs any absolute positioning error from the linear transportation machine, then the entire precision from either the drilling, welding or screwing process is bound to deteriorate, and the entire performance will be affected. The entire processing task even collapses if the absolute tracking error from any process fails.

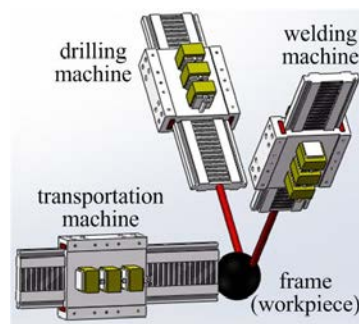


Figure 1. Coordination of linear machines.

If each linear processing machine is formed as the control object and it has the controller, sensor, and drives of its own, then multiple linear machines based local motion control system can be considered as a multi-agent system. By using appropriate coordination control laws, the linear machines can be coupled to form a united coordination network [2]. For example, the ultimate global tracking goal of the automobile frame assembly process can thus be accomplished by the interactive local controllers from the linear machines, without requiring any supervisory administration or decision [3]. As one type of direct-drive linear actuators, the linear switched reluctance machine (LSRM) possesses a robust and stable machine structure, and it is more suitable for the construction of a distributed control network [4]. The arrangement of multiple LSRMs working in a coordinated manner ensures a faster processing speed since all machines can work together instead of waiting for others to finish [5].

In the leader–follower LSRM network, only the leader LSRM straightly accesses the reference signal, and all follower machines track the reference signal by either directly or indirectly following the leader machine, which is determined by some communication topology [6]. The relative tracking precision of any two interactive LSRMs can be guaranteed with the introduction of appropriate coordinated control laws of the LSRM network [7]. It is clear that the overall tracking precision for the coordinated LSRM network includes the relative precision from all followers to the leader and also the absolute precision from the leader LSRM concerning the reference signal.

To ensure the overall precision of the automobile frame assembly process, for example, the absolute precision from the reference to the leader LSRM and the relative tracking accuracy among the follower LSRMs should also be satisfied. However, it is not always applicable to access the reference for all nodes due to the engineering practice consideration, such as system cost and complexity. Practically, only part of the node (leader) is involved in receiving the reference signal, while other nodes (followers) cannot form a direct closed loop link, according to Reference [8].

The above leader–follower network is inspired by the collective evasion or migration phenomenon of animal group motion, such as fish schooling and birds flocking, where the minority individuals can perceive any predators threaten or transfer path only, and the collective monolithic behavior is generated through the topology of the information propagation and exchange [9]. Such collective behavior can be modeled as a dynamical, target-driven, tracking network and it has the characteristic that the motion of the leader is independent of the followers [10]. The principle of the information exchange among the individuals is primarily formulated as a consensus protocol. The consensus algorithm with a distributed extended state observer is designed for the leader–follower network composed of multi-agents with general linear dynamics and unknown external disturbances [11]. The methodology to design the feedback control laws on all the followers is proposed, and the method contains an adjustable parameter for tracking the leader semi-globally [12]. Based on general high-order distributed consensus protocols, a leader–follower control problem is studied to reveal that the agents with small degrees should be selected as leaders to reach consensus [13]. A flocking algorithm combined with the consensus and attraction/repulsion function is implemented for the

robotic fish leader–follower network to enable follower fish to track the leader fish to reach the desired destination [6]. The formation control of multiple mobile robots based leader–follower network is investigated by [14] and a reputation-based, distributed control algorithm is introduced for the leader–follower consensus network in the presence of misbehaving agents [15].

The absolute precision of the LSRM network is difficult to be guaranteed by applying the coordinated control laws solely, with the nonexistence of a global feedback mechanism. If there are specific tracking errors from the leader respective to the reference, then such errors are bound to be transmitted to the followers through the physical link from the communication topology. The lack of direct feedback mechanism from followers to the reference inevitably results in the fact that the errors cannot be further corrected. As a result, a global feedback strategy should be developed for the LSRM network for the improvement of both the absolute and relative precision. It is natural that the global full-state feedback control structure should be constructed for the improvement of the overall accuracy of the proposed LSRMs leader–follower network. The controllability and the observability of the network should first be satisfied before any proper design of the global feedback controller and observer, respectively.

In recent years, there has been a surge of activities discussing how communication topology and selected leaders affect the fundamental properties of network controllability [16–18]. The observability and controllability are dual concepts mathematically. Both concepts were extensively explored and provided many useful theorems [19–21]. The controllability of the leader–follower network can be classified into three classes: fully controllable, completely uncontrollable, and conditionally controllable [22]. A graph-theoretical characterization of controllability and observability for a leader–follower network is developed over the finite fields so that the quantized agents can be put into any desired configuration by a set of leader agents [23]. The relationship between the network topology and the controllability of the network containing a single leader is discussed, and some key results in this area are summarized [24]. The controllability and observability of a network with hybrid linear agents are investigated, and some necessary and sufficient conditions are derived from the Popov–Belevitch–Hautus (PBH) test [25]. The analysis of the structural mechanism of controllability for the leader selection is provided under different assumptions, and a structural characterization of all the solutions is provided [26].

It is evident that both the global controller and observer can be designed to be located on the leader. If only one LSRM node is selected as both the leader and the observer, the computation burden is increased for the node, and meanwhile, the controllability and observability of the network are hard to be guaranteed. To fully utilize the communication links to participate the global feedback control framework of the LSRM network, the global controller and observer can be separately deployed onto either the leader or the follower for independent control and state observation, respectively [27].

From the above analysis, this article first proposes a leader–follower–observer network for three LSRMs to realize coordinated tracking, targeting to the potential applications in the assembly field. The leader is responsible for the global control, and the observer is applied for full-state observation, and they are allocated separate LSRM nodes, respectively. Next, the internal model compensator (IMC) combined with the full-state feedback controller, which acquires the full states reconfigured by the observer, is applied to improve the coordinated tracking accuracy. To ensure the realizability of the global feedback controller, we discuss the controllability of the LSRM network with the IMC. Consequently, the inherent controllability of the LSRM network is a critical condition of the controllability of the LSRM network with the IMC. Therefore, the controllability and the observability of the LSRM network are then inspected. Experimentation verifies the effectiveness of the proposed network control scheme and the results prove that both the absolute and the relative accuracy can be guaranteed by the proposed method.

The contributions include the following. First, the coordinated tracking of a leader–follower–observer LSRM network is proposed and investigated, with the separation of the global controller and the observer. Second, the controllability of the proposed LSRM network with the IMC is discussed

for a proper design of the global controller. Third, design and implementation of the global controller are performed for the LSRM network. The relationship of network topology with IMC and network controllability is analyzed from the perspective of network though the control objects are linear systems. Meanwhile, the configuration for leader and observer is derived. The methodology can also be extended to other networked systems.

2. Notations and Theoretical Background

The LSRM network is composed of N homogeneous LSRMs modeled as linear time-invariant dynamics. The interior adhesion effect of the LSRM network is produced by the consensus algorithm distributed on each LSRM node, and each node exchanges state information with others through the communication network.

2.1. Concept of Graph Theory

The communication network can be modeled as a graph $\mathcal{G} = (\mathcal{V}, \mathcal{E})$. \mathcal{V} represents the set of nodes, in which the node $v_i \in \mathcal{V}, i = 1, \dots, N$ refers to the i -th LSRM unit. $\mathcal{E} \subseteq \mathcal{V} \times \mathcal{V}$ denotes the set of edges. $e_{ij} = (v_i, v_j) \in \mathcal{E}$ indicates a communication links existing from v_j to v_i .

Let $\mathbb{R}^{n \times m}$ be the sets of the real $n \times m$ matrix. A graph \mathcal{G} can be denoted as an adjacency matrix $\mathcal{A} \in \mathbb{R}^{N \times N}$ with each entry $a_{ij} > 0, i, j = 1, \dots, N$ if and only if $e_{ij} \in \mathcal{E}$, otherwise $a_{ij} = 0$. The Laplacian matrix $\mathcal{L} \in \mathbb{R}^{N \times N}$ is defined as follows:

$$\mathcal{L} = \mathcal{D} - \mathcal{A} \quad (1)$$

where $\mathcal{D} = \text{diag}\{d_i\} \in \mathbb{R}^{N \times N}, i = 1, \dots, N$ is the diagonal in-degree matrix with $d_i = \sum_{j=1}^N a_{ij}$ the degree of node i (i.e., the i -th row sum of \mathcal{A}).

2.2. Leader–Follower–Observer Network

The behaviors of the N LSRMs are coupled by the effect of the distributed controller based the consensus algorithm using the communication network depicted as \mathcal{G} . As a result, the N LSRMs are bound as the LSRM network. As shown in Figure 2, for the network composed of three LSRMs, LSRM 1 is called the leader, and it can receive the reference signal, which can be defined as the input of the LSRM network. LSRM 3 is termed as the observer, and its output is the output of the network. The other LSRM node (LSRM 2) can be neither observed nor controlled outside the network, termed as a follower. The network composed of the leader, follower and observer is termed a leader–follower–observer network.

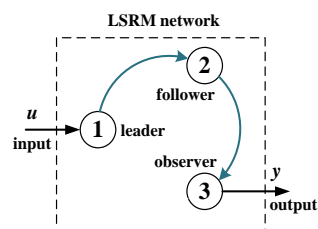


Figure 2. LSRMs leader–follower–observer network.

To form the LSRM network, we employ the consensus algorithm as the distributed controller, which is allocated on each LSRM node, to coordinate the states of the N LSRMs. Therefore, the consensus algorithm for a network composed of N LSRMs is formulated as follows [28],

$$\mathbf{u}_i = f \left[\sum_{j=1}^N a_{ij} \cdot g(x_i - x_j) \right], \forall x_i(0), x_j(0), i, j = 1, \dots, N \quad (2)$$

to realize,

$$\begin{cases} \lim_{t \rightarrow \infty} (x_i - x_j) = 0 \\ \lim_{t \rightarrow \infty} (\dot{x}_i - \dot{x}_j) = 0 \end{cases} \quad (i \neq j)$$

where x_i is the state of the i -th LSRM, including the position and velocity information.

2.3. Notation Preliminaries and Problem Statements

Superscript T denotes the transpose of a real matrix. I_N represents the identity matrix of dimension N , $\mathbf{0}$ indicates a zero matrix of an appropriate dimension. N_i denotes the neighbor LSRMs set of the i -th LSRM, i.e., it can receive the states of the N_i LSRM nodes. Subscript l, f, o represent the selected nodes for the leader, follow and observer, respectively. $\dim(\cdot)$ is the dimension of a vector or matrix. The Kronecker product of two matrices $M \in \mathbb{R}^{n \times m}$, $N \in \mathbb{R}^{p \times q}$ denoted by $M \otimes N$ is defined as the $np \times mq$ matrix [29],

$$M \otimes N = \begin{bmatrix} m_{11}N & \cdots & m_{1n}N \\ \vdots & \ddots & \vdots \\ m_{m1}N & \cdots & m_{mn}N \end{bmatrix} \quad (3)$$

The following property is satisfied with the Kronecker product,

$$\begin{aligned} (A \otimes B)(C \otimes D) &= (AC) \otimes (BD) \\ (A + B) \otimes C &= A \otimes C + B \otimes C \\ k(A \otimes B) &= (kA) \otimes B = A \otimes (kB) \\ (A \otimes B)^T &= A^T \otimes B^T \end{aligned}$$

where A, B, C, D represent the matrices with the appropriate dimensions, and k denotes a scalar value.

According to the proposed LSRM network adopted by this paper, the following reasonable assumptions are made to restrict the scope of the study.

Assumption 1. All LSRM nodes are homogeneous without the mechanical or electrical difference and the controllability, observability, and stability can be satisfied.

Assumption 2. There is a sole LSRM as the leader receiving the control input from the outside of the network, and another sole LSRM can be observed externally, as shown in Figure 2. In addition, the distributed control law can receive the full-state information of all neighbor LSRM nodes through the communication network.

3. Modeling of the LSRMs Network

The dynamics for a typical LSRM is governed by the following dynamic equation [30],

$$m_i \cdot \frac{d^2 x_i}{dt^2} + B_i \cdot \frac{dx_i}{dt} + f_i = F_i \quad (4)$$

where m_i , B_i , x_i , f_i and F_i are the mass, friction coefficient, position, load force and the generated propulsion force, respectively. Rearranging Equation (4) in the state-space form, we have,

$$\begin{bmatrix} \dot{x}_i \\ \ddot{x}_i \end{bmatrix} = \begin{bmatrix} 0 & 1 \\ 0 & -\frac{B_i}{m_i} \end{bmatrix} \begin{bmatrix} x_i \\ \dot{x}_i \end{bmatrix} + \begin{bmatrix} 0 \\ \frac{1}{m_i} \end{bmatrix} u_i \quad (5)$$

Let $x_i = [x_i, \dot{x}_i]^T$, we have $A_i = \begin{bmatrix} 0 & 1 \\ 0 & -\frac{B_i}{m_i} \end{bmatrix}$ and $B_i = \begin{bmatrix} 0 \\ \frac{1}{m_i} \end{bmatrix}$. Equation (5) can be represented in the state-space as,

$$\dot{x}_i = A_i x_i + B_i u_i \quad (6)$$

where $u_i = F_i - f_i$.

The N LSRMs can be formulated as,

$$\begin{bmatrix} \dot{x}_1 \\ \vdots \\ \dot{x}_N \end{bmatrix} = \begin{bmatrix} A_1 & \cdots & \mathbf{0} \\ \vdots & \ddots & \vdots \\ \mathbf{0} & \cdots & A_N \end{bmatrix} \begin{bmatrix} x_1 \\ \vdots \\ x_N \end{bmatrix} + \begin{bmatrix} B_1 & \cdots & \mathbf{0} \\ \vdots & \ddots & \vdots \\ \mathbf{0} & \cdots & B_N \end{bmatrix} \begin{bmatrix} u_1 \\ \vdots \\ u_N \end{bmatrix} \quad (7)$$

Since all the LSRMs are identical according to Assumption 1, all the subscripts for A_i, B_i, K_i can be neglected as,

$$\dot{x} = I_N \otimes Ax + I_N \otimes Bu \quad (8)$$

Based on the second-order consensus algorithm, the distributed controller for the i -th LSRM is depicted as [13],

$$u_i = \sum_{j=1}^N a_{ij} \begin{bmatrix} K_{p,i} & K_{d,i} \end{bmatrix} \begin{bmatrix} x_j(t) - x_i(t) \\ \dot{x}_j(t) - \dot{x}_i(t) \end{bmatrix} \quad (9)$$

where $K_{p,i}$ and $K_{d,i}$ are the gains of the distributed controller. The distributed controller of the N LSRMs is represented in the matrix form as,

$$u = -(\mathcal{L} \otimes K)x \quad (10)$$

with $K = \begin{bmatrix} K_{p,i} & K_{d,i} \end{bmatrix}$. Substituting Equation (10) into Equation (8), we obtain,

$$\begin{aligned} \dot{x} &= I_N \otimes Ax - (I_N \otimes B)(\mathcal{L} \otimes K)x \\ &= (I_N \otimes A - \mathcal{L} \otimes BK)x \end{aligned} \quad (11)$$

The Equation (11) is the dynamics of the LSRM network without considering leader and observer.

For the leader–follower–observer LSRM network proposed in Figure 2, since the leader is driven by the control input u , the leader dynamics can be expressed as,

$$\dot{x}_l = Ax_l + \sum_{j=1}^N a_{lj} BK(x_j(t) - x_l(t)) + Bu \quad (12)$$

Here, the states of the leader are denoted as x_l .

Since the follower is only driven by the LSRMs node internally from the network, the follower dynamics can be represented as,

$$\dot{x}_f = Ax_f + \sum_{j=1}^N a_{fj} BK(x_j(t) - x_f(t)) \quad (13)$$

Here, the states of the follower are denoted as x_f . The observer can thus be expressed as,

$$\begin{cases} \dot{x}_o = Ax_o + \sum_{j=1}^N a_{oj} BK(x_j(t) - x_o(t)) \\ y = Cx_o \end{cases} \quad (14)$$

where the states of the observer are x_o . Equations (12)–(14) constitute the complete dynamics of the leader–follower–observer LSRM network, and the LSRM network dynamics can thus be derived as

$$\begin{aligned} \dot{x} &= (I_N \otimes A - \mathcal{L} \otimes BK)x + (\mathcal{B} \otimes B)u \\ y &= (\mathcal{C} \otimes C)x \end{aligned} \tag{15}$$

where C is the output matrix of the LSRM node; and $\mathcal{B} = \begin{bmatrix} 1 & 0 & 0 \end{bmatrix}^T$ and $\mathcal{C} = \begin{bmatrix} 0 & 0 & 1 \end{bmatrix}$, which denote the input and output matrix of the communication network, respectively. y is the output of the LSRM network. The overall control diagram of the proposed leader–follower–observer LSRM network can thus be represented in Figure 3.

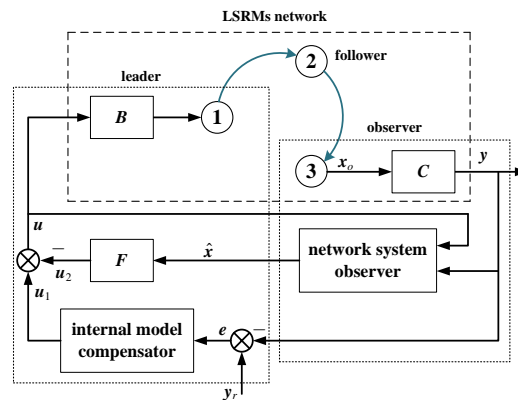


Figure 3. Control diagram of LSRM network.

4. LSRMs Network with IMC

4.1. Internal Model Compensator Design

To realize a zero-offset tracking performance, the following equation for the LSRM network holds [27],

$$\lim_{t \rightarrow \infty} e(t) = \lim_{t \rightarrow \infty} [y(t) - y_r(t)] = 0 \tag{16}$$

The transfer function of reference signal $y_r(t)$ can be derived by Laplace transform as,

$$Y_r(s) = \frac{n(s)}{d(s)} \tag{17}$$

where $n(s)$ and $d(s)$ depict the quantitative and structural characteristics of the reference signal at frequency domain, respectively. $d(s)$ can be decomposed into two parts as follows,

$$d(s) = \bar{\phi}(s)\phi(s) \tag{18}$$

where $\bar{\phi}(s)$ is the stable part, while $\phi(s)$ is the unstable part and it can be represented as,

$$\phi(s) = s^l + a_{l-1}s^{l-1} + \dots + a_1s + a_0 \tag{19}$$

Here, $a_i (i = 0, \dots, l - 1)$ are the coefficients of the l -th order unstable part. According to Equation (19), the unstable model of the reference signal $y_r(t)$ is derived as,

$$\begin{cases} \dot{x}_r = A_r x_r \\ y_r = C_r x_r \end{cases} \tag{20}$$

where $A_r = \begin{bmatrix} 0 & & & \\ \vdots & & I_{l-1} & \\ 0 & & & \\ -a_0 & -a_1 & \cdots & -a_{l-1} \end{bmatrix}$ and $C_r = [1 \ 0 \ \cdots \ 0]$.

Moreover, x_r is the states of the IMC. Further, the IMC can be designed as follows [31],

$$\begin{cases} \dot{x}_r = A_r x_r + B_r e \\ u_1 = F_r x_r \\ e(t) = y_r(t) - y(t) \end{cases} \tag{21}$$

where F_r is the gain matrix of the compensator, u_1 is the control output of the IMC, and $B_r = [0 \ 0 \ \cdots \ 1]^T$. If the reference signal y_r is sinusoidal, x_r can be represented as,

$$\dot{x}_r = \begin{bmatrix} 0 & 1 \\ -\omega^2 & 0 \end{bmatrix} x_r + \begin{bmatrix} 0 \\ 1 \end{bmatrix} \cdot [y_r(t) - y(t)] \tag{22}$$

The IMC thus can be illustrated in Figure 4.

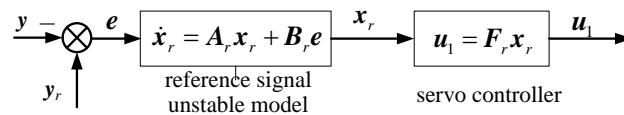


Figure 4. Internal model compensator (IMC) structure.

The network dynamics incorporating the IMC can thus be represented as,

$$\begin{bmatrix} \dot{x} \\ \dot{x}_r \end{bmatrix} = \begin{bmatrix} I_N \otimes A - \mathcal{L} \otimes BK & \mathbf{0}_{Nn \times l} \\ -B_r(\mathcal{C} \otimes C) & A_r \end{bmatrix} \begin{bmatrix} x \\ x_r \end{bmatrix} + \begin{bmatrix} \mathcal{B} \otimes B \\ \mathbf{0}_{l \times Pp} \end{bmatrix} u + \begin{bmatrix} \mathbf{0}_{Nn \times 1} \\ B_r \end{bmatrix} y_r \tag{23}$$

According to the structure of the LSRM network, as shown in Figure 3, the control input is the state feedback of Equation (23), which is denoted as,

$$u = - \begin{bmatrix} F & -F_r \end{bmatrix} \begin{bmatrix} \hat{x} \\ x_r \end{bmatrix} \tag{24}$$

where F is the gain matrix of the state feedback, as shown in Figure 3.

It is clear that the necessary and sufficient condition for the existence of state feedback in Equation (24) is that the network depicted as Equation (23) should be fully controllable.

4.2. Controllability of LSRMs Network with IMC

Theorem 1. The sufficient condition for the controllability of Equation (23) is satisfied,

1. The LSRM network ($I_N \otimes A - \mathcal{L} \otimes BK, \mathcal{B} \otimes B$) is fully controllable.
2. (A_r, B_r) of the IMC is a controllable matrix pair.
3. The LSRM network with the IMC should be satisfied by that.
4. All roots γ_i of the unstable equation $\phi(s) = 0$ of y_r should satisfy.

$$\text{rank} \begin{bmatrix} \gamma_i I_{Nn} - (I_N \otimes A - \mathcal{L} \otimes BK) & \mathcal{B} \otimes B \\ -\mathcal{C} \otimes C & \mathbf{0}_{Qq \times Pp} \end{bmatrix} = Nn + Qq, i = 1, \dots, l \tag{25}$$

Proof of Theorem 1. According to the PBH criteria, if Equation (23) is fully controllable, then the following equation can be satisfied as,

$$\begin{aligned}
 & \text{rank}W_{(Nn+l) \times (Nn+l+Pp)}(s) \\
 &= \text{rank} \begin{bmatrix} sI_{Nn} - (I_N \otimes A - \mathcal{L} \otimes BK) & \mathbf{0}_{Nn \times l} & \mathcal{B} \otimes B \\ \mathbf{B}_r(\mathcal{C} \otimes C) & sI_l - A_r & \mathbf{0}_{l \times Pp} \end{bmatrix} \\
 &= \text{rank} \begin{bmatrix} sI - (I_N \otimes A - \mathcal{L} \otimes BK) & \mathcal{B} \otimes B & \mathbf{0}_{Nn \times l} \\ \mathbf{B}_r(\mathcal{C} \otimes C) & \mathbf{0}_{l \times Pp} & sI - A_r \end{bmatrix} \\
 &= Nn + l
 \end{aligned} \tag{26}$$

where N, n are the dimensions of \mathcal{A} associated with graph \mathcal{G} and the system matrix of each LSRM node, respectively. P, p are the dimensions of \mathcal{B} and the input matrix B of each LSRM node, respectively. Q, q are the dimensions of \mathcal{C} and the output matrix C of each LSRM node, respectively.

First, except for the roots of $\phi(s) = 0$, $\text{rank}W(s) = Nn + l$ is proven. Supposing that Equation (25) holds, i.e., the LSRM network from Equation (15) is fully controllable, according to the PBH criteria, we have,

$$\text{rank} \begin{bmatrix} sI_{Nn} - (I_N \otimes A - \mathcal{L} \otimes BK) & \mathcal{B} \otimes B \end{bmatrix} = Nn \tag{27}$$

Regarding the structure of A_r , we have,

$$\text{rank}[sI_l - A_r] = l, \forall \phi(s) \neq 0 \tag{28}$$

Combing Equations (27) and (28), we have

$$\text{rank}W(s) = Nn + l, \forall \phi(s) \neq 0 \tag{29}$$

Second, for the roots of $\phi(s) = 0$, $\text{rank}W(s) = Nn + l$, $W(s)$ can be represented as,

$$\begin{aligned}
 W(s) &= \begin{bmatrix} sI_{Nn} - (I_N \otimes A - \mathcal{L} \otimes BK) & \mathbf{0}_{Nn \times l} & \mathcal{B} \otimes B \\ \mathbf{B}_r(\mathcal{C} \otimes C) & sI_l - A_r & \mathbf{0}_{l \times Pp} \end{bmatrix} \\
 &= \begin{bmatrix} I_{Nn} & \mathbf{0}_{Nn \times 1} & \mathbf{0}_{Nn \times l} \\ \mathbf{0}_{l \times Nn} & -B_r & -(sI_l - A_r) \end{bmatrix} \times \\
 &\quad \begin{bmatrix} sI_{Nn} - (I_N \otimes A - \mathcal{L} \otimes BK) & \mathbf{0}_{Nn \times l} & \mathcal{B} \otimes B \\ -(\mathcal{C} \otimes C) & \mathbf{0}_{Qq \times l} & \mathbf{0}_{Qq \times Pp} \\ \mathbf{0}_{l \times Nn} & I_l & \mathbf{0}_{l \times Pp} \end{bmatrix}
 \end{aligned} \tag{30}$$

From the condition of full controllability of (A_r, B_r) , we have,

$$\text{rank} \begin{bmatrix} I_{Nn} & \mathbf{0}_{Nn \times 1} & \mathbf{0}_{Nn \times l} \\ \mathbf{0}_{l \times Nn} & -B_r & -(sI_l - A_r) \end{bmatrix} = Nn + l \tag{31}$$

According to Conditions 3 and 4 from Theorem 1,

$$\begin{aligned}
 & \text{rank} \begin{bmatrix} sI_{Nn} - (I_N \otimes A - \mathcal{L} \otimes BK) & \mathbf{0}_{Nn \times l} & \mathcal{B} \otimes B \\ -(\mathcal{C} \otimes C) & \mathbf{0}_{Qq \times l} & \mathbf{0}_{Qq \times Pp} \\ \mathbf{0}_{l \times Nn} & I_l & \mathbf{0}_{l \times Pp} \end{bmatrix} \\
 &= Nn + Qq + l
 \end{aligned} \tag{32}$$

By applying the Sylvester Inequality, we have,

$$\text{rank}H + \text{rank}V - \beta \leq \text{rank}HV \leq \min\{\text{rank}H, \text{rank}V\} \tag{33}$$

where H and V are the $\alpha \times \beta$ matrix and $\beta \times k$ matrix, respectively. For the LSRM network from Equation (15), the following equation holds,

$$\begin{aligned} Nn + l &= (Nn + l) + (Nn + Qq + l) - (Nn + Qq + l) \leq \text{rank}W(s) \\ &\leq \min\{(Nn + l), (Nn + Qq + l)\} = Nn + l \end{aligned} \quad (34)$$

Then, we have,

$$\text{rank}W(s) = Nn + l, \text{ for any root of } \forall \phi(s) = 0 \quad (35)$$

Combining Equations (29) and (35), we have

$$\text{rank}W(s) = Nn + l \quad (36)$$

In other words, the LSRM network incorporating the IMC denoted in (23) is fully controllable. Theorem 1 is proven. \square

Remark 1. From the four necessary Conditions 1–4 in Theorem 1, Conditions 2–4 can be realized by the proper configuration of the input and output of the LSRM network, together with the suitable selection of the reference signal and IMC design. Therefore, condition 1 becomes the crucial element to guarantee the full controllability of Equation (23). It is clear that the controllability of the LSRM network in [31] without the IMC should first be satisfied, which is equivalent to the fact that $I_N \otimes A - c\mathcal{L} \otimes BK$ and $\mathcal{B} \otimes B$ consist of a controllable matrix pair. Unfortunately, the classic Kalman rank criteria of the linear system [31] are not able to illustrate the essential relationship between the controllability of the LSRM network Equation (15) and the controllability of the LSRM node (A, B) (termed as a physical system) together with the coordinated network $(\mathcal{L}, \mathcal{B})$ (termed as a cyber system) in Equation (15).

A controllability criteria of the LSRM network derived in [32] can be employed for revealing the controllability condition of the LSRM network Equation (15).

Theorem 2. In [32], if both the coordinated network $\{\mathcal{L}, \mathcal{B}\}$ (the i -th eigenvalue of the matrix denotes λ_i) and the local closed-loop system $\{A - \lambda_i BK, B\}$ of the LSRM node i are controllable, the LSRM network as $I_N \otimes A - c\mathcal{L} \otimes BK$ is controllable.

Proposition 1. The LSRM network is observable, if and only if both $(\mathcal{L}, \mathcal{C})$ and $\{A - \lambda_i BKC, C\}$ are the observable matrix pairs.

Since controllability and observability are dual, Proposition 1 can be proven similarly. It is clear that the controllability $\{A - \lambda_i BK, B\}$ can be guaranteed for any LSRM node according to the LSRM characteristics and the local controller of the distributed control law. Referring to the communication topology as shown in Figure 2, the selection of LSRM 1 (leader) and LSRM 3 (observer) ensures that $(\mathcal{L}, \mathcal{B})$ is fully controllable.

5. Global Controller and Observer Design

5.1. Controller Design

According to Theorem 1, the proposed controller Equation (24) with IMC and state feedback is designed by the linear quadratic regular method, and the cost function is defined as [31],

$$J = \int_0^{\infty} (\tilde{x}^T Q_{\tilde{x}} \tilde{x} + u^T Q_u u) dt \quad (37)$$

Here, $\tilde{x} = \begin{bmatrix} \hat{x}^T & x_r^T \end{bmatrix}^T$, $Q_{\tilde{x}} \in \mathbb{R}^{(Nn+l) \times (Nn+l)} \geq 0$ and $Q_u \in \mathbb{R}^{Pp \times Pp} \geq 0$ are symmetric, positive or semi-positive definite matrices. The feedback gain matrix can be solved as,

$$u = -Q_u^{-1} \tilde{B}^T P \tilde{x} \tag{38}$$

where $\tilde{B} = \begin{bmatrix} B^T \otimes B^T & 0_{l \times 1} \end{bmatrix}^T$, the matrix $P \in \mathbb{R}^{(Nn+l) \times (Nn+l)}$ is a positive definite, symmetric matrix that satisfies the algebraic Riccati equation as,

$$PA + A^T P - P \tilde{B} Q_u^{-1} \tilde{B}^T P + Q_x = 0 \tag{39}$$

According to Equation (24), the control gain matrix is composed of two parts, that is to say, $-F$ and F_r . The gain matrix can thus be obtained as,

$$\begin{cases} F = [Q_u^{-1} \tilde{B}^T P]_{Pp \times Nn} \\ F_r = [-Q_u^{-1} \tilde{B}^T P]_{Pp \times l} \end{cases} \tag{40}$$

As a result, the IMC and the feedback controller are depicted as,

$$\begin{cases} \dot{x}_r = A_r x_r + B_r e \\ u_1 = F_r x_r \\ u_2 = F \hat{x} \end{cases} \tag{41}$$

5.2. Observer Design

The observer structure of the LSRM network with IMC is illustrated as shown in Figure 5. Feedback is derived from the term $L(y - (C \otimes C)\hat{x})$, which is proportional to the difference between the observed output y and the output predicted by the observer \hat{y} .

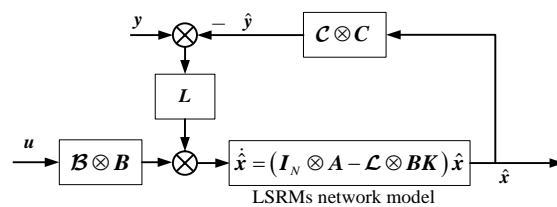


Figure 5. Observer structure.

The observer can thus be depicted as,

$$\dot{\hat{x}} = (I_N \otimes A - L \otimes BK)\hat{x} + L(y - \hat{y}) + (B \otimes B)u \tag{42}$$

Define the estimation error $x_e = x - \hat{x}$, and the following equation can be obtained from Equation (42) as,

$$\dot{x}_e = [(I_N \otimes A - L \otimes BK) - L(C \otimes C)]x_e \tag{43}$$

Consequently, the closed loop system is thus governed by,

$$\begin{aligned} \begin{bmatrix} \dot{x} \\ \dot{x}_r \\ \dot{x}_e \end{bmatrix} &= A_c \begin{bmatrix} x \\ x_r \\ x_e \end{bmatrix} + \begin{bmatrix} \mathbf{0}_{Nn \times 1} \\ \mathbf{B}_r \\ \mathbf{0}_{Nn \times 1} \end{bmatrix} y_r \\ y &= \begin{bmatrix} \mathbf{C} \otimes \mathbf{C} & \mathbf{0}_{Qq \times (Nn+l)} \end{bmatrix} \begin{bmatrix} x \\ x_r \\ x_e \end{bmatrix} \end{aligned} \quad (44)$$

where $A_c = \begin{bmatrix} A_{c,11} & A_{c,12} \\ A_{c,21} & A_{c,22} \end{bmatrix}$, and $A_{c,11} = \begin{bmatrix} I_N \otimes A - \mathcal{L} \otimes BK - (\mathcal{B} \otimes B)F & (\mathcal{B} \otimes B)F_r \\ -B_r(\mathbf{C} \otimes \mathbf{C}) & A_r \end{bmatrix}$, $A_{c,12} = \begin{bmatrix} (\mathcal{B} \otimes B)F \\ \mathbf{0}_{Nn \times Nn} \end{bmatrix}$, $A_{c,21} = \mathbf{0}_{Nn \times (Nn+l)}$, $A_{c,22} = I_N \otimes A - \mathcal{L} \otimes BK - L(\mathbf{C} \otimes \mathbf{C})F$.

5.3. Control Algorithms of Leader, Follower, and Observer

According to Figure 2, the control equation of the leader allocated at LSRM 1 is derived as,

$$\begin{cases} \dot{x}_l = Ax_l + \sum_{j \in N_l} BK(x_l - x_j) - BF\hat{x} + BF_r x_r \\ \dot{x}_r = A_r x_r + B_r [y_r - (\mathbf{C} \otimes \mathbf{C})x] \end{cases} \quad (45)$$

From Equation (9), the consensus control law is applied to the control structure of the follower, namely, LSRM 2, as follows,

$$\dot{x}_f = I_{N-2} \otimes Ax_f + \sum_{j \in N_f} BK(x_f - x_j) \quad (46)$$

LSRM 3 is implemented as the observer which provides the estimated state information of the LSRM network. The control structure of the LSRM 2 is thus formulated as,

$$\begin{cases} \dot{x}_o = Ax_o + \sum_{j \in N_o} BK(x_o - x_j) \\ \dot{\hat{x}} = [I_N \otimes A - \mathcal{L} \otimes BK - L(\mathbf{C} \otimes \mathbf{C}) - (\mathcal{B} \otimes B)F]\hat{x} \\ \quad + Ly + (\mathcal{B} \otimes B)F_r x_r \\ y = (\mathbf{C} \otimes \mathbf{C})x \end{cases} \quad (47)$$

6. LSRMs Network Construction

6.1. LSRM Node

The machine topology is depicted as shown in Figure 6a–c and all LSRMs adopt the asymmetric and double-sided structure to achieve a more stable and reliable output performance [27]. Each LSRM is composed of six stators with windings that form phase aa', bb' and cc'. Both the phases and the mover's teeth are not perfectly mirrored according to the axis. Compared to a double-sided, symmetric counterpart with the same dimensions and ratings, such machine arrangement ensures a higher force-to-volume ratio with more acceleration [27]. The LSRMs can be regarded as identical control objects with the same dimensions and ratings. Major machine specifications can be found in Table 1.

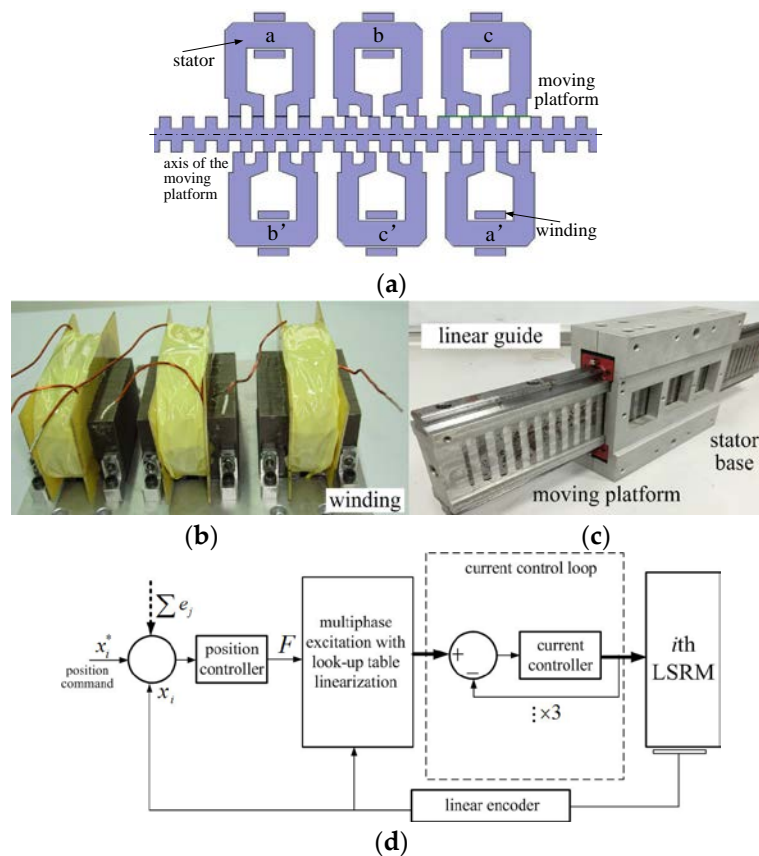


Figure 6. (a) Schematic of LSRMs; (b) stator and windings; (c) stator base and moving platform; and (d) LSRM control diagram.

Table 1. Major Specifications of LSRMs.

Parameter	Value
mass of moving platform	3.8 kg
pole width	6 mm
pole pitch	12 mm
phase resistance	2 ohm
air gap length	0.3
number of turns	160
stack length	50 mm

The position control diagram of the single LSRM can be represented in Figure 6d. The dual-loop control strategy with current as the inner loop and position as the outer loop is adopted [33]. The multi-phase excitation with look-up table linearization scheme is employed to combat the nonlinearities of the LSRMs [33]. The current control loop is faster enough to regulate the actual current output for each phase with proper response time and precision. For the i -th LSRM node, the position error e_i is decided from the difference between the command x_i^* and the actual position x_i of i -th LSRM, along with the difference information from the j -th machine e_j . The position controller then calculates the control input f_j , and the multi-phase excitation with the look-up table linearization scheme determines the current command for the k -th winding, according to the current position of the machine.

6.2. Construction of LSRMs Network

The overall structure of the position network is illustrated in Figure 7. The communication network topology depicted in Figure 2 is applied. The communication interface represents the communication hardware and protocol to access other LSRM nodes. The communication framework is composed of two parts: the network topology and the feedback path which is bidirectional. The estimated states and the output signals of the LSRM network are delivered from the observer to the leader, and the control input signal is transmitted from the leader to the observer through the feedback path simultaneously. The control input signal is applied to construct the full states of the LSRM network.

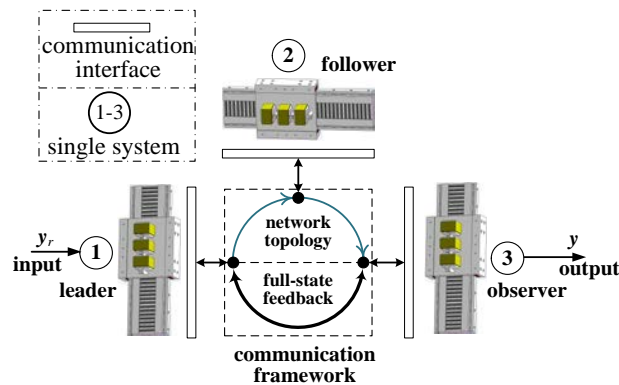


Figure 7. Hardware construction of LSRM network.

7. Experimental Results

7.1. Experimental Setup

The experimental setup, such as the controller platforms, drivers, and power supply, can be found in Figure 8a. Every LSRM node includes one (Advanced RISC Machine) ARM development kit, one three-channel digital-to-analog (DA) module, three current drivers and a sensor interface circuit. The real-time position information from the linear magnetic encoder is collected by the sensor interface circuit and transmitted to the ARM board. The current drivers are three commercial amplifiers that are capable of internal current regulation of a sampling rate of 20 kHz with precise current control performance. The LSRMs can be found in Figure 8b with identical dimensions and ratings. The LSRMs can be mounted onto any required mechanism to perform the appropriate coordinated operation, as illustrated in Figure 1.

Communication among every single system is realized by the controller area network (CAN) protocol with a baud rate of 1 Mbps with 32-bit data transmission. A supervising personal computer (PC) is used to transmit the control signal to the leader LSRM and collect state information in real time, by the serial ports from ARM platforms. The communication is realized by the serial port with the RS232 protocol from the leader to the PC, and the baud rate is 115,200 with data and stop bit set as 8 and 1, respectively.

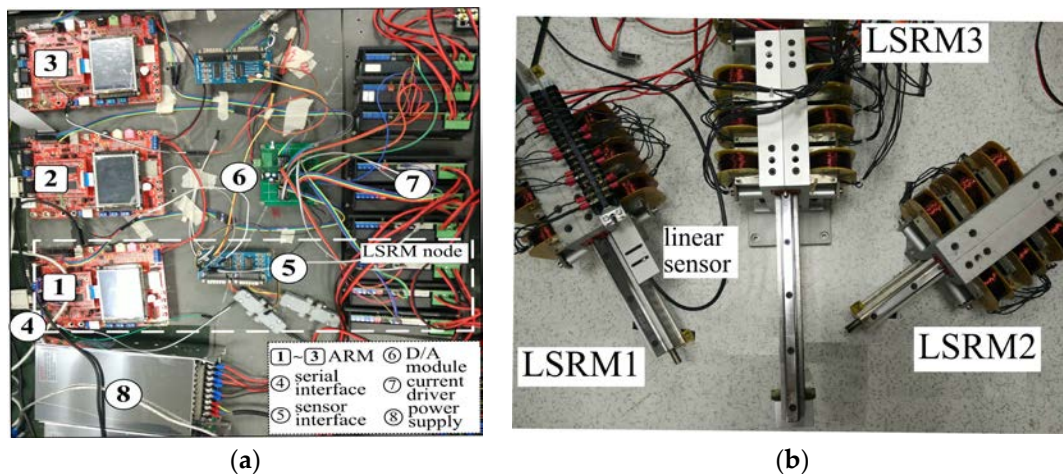


Figure 8. Experimental setup: (a) control platforms and drivers; and (b) LSRMs.

7.2. Control Parameter Derivations

The expected poles and the position and velocity control gains are configured as tabulated in Table 2. The gains of the controller and the observer can then be calculated, according to Equations (24) and (40). The gains are tabulated in Table 2. $Q_{\bar{x}}$ and Q_u are selected as $I_{8 \times 8}$ and 1, respectively. The gains of the consensus algorithm from Equation (9) are selected as $K_{p,i} = 2$ and $K_{d,i} = 0.02$, respectively [31].

Table 2. Controller and observer gain and parameters.

Parameter	Controller	Observer
Gain	$F = \begin{bmatrix} 28.1329 \\ 37.2800 \\ 99.5444 \\ 110.7767 \\ 184.4060 \\ 221.7721 \end{bmatrix}^T$ $F_r = \begin{bmatrix} -10.3000 \\ -38.3000 \end{bmatrix}^T$	$L = \begin{bmatrix} -305.2473 \\ 192.2114 \\ -448.938 \\ 399.5258 \\ 44.9560 \\ 596.1126 \end{bmatrix}$

7.3. Experimental Results and Analysis

The reference signal is the sinusoidal waveform with the amplitude of 30 mm, and the frequency value is 0.2 Hz. The tracking response waveforms for the LSRM network with only the consensus algorithm can be found in Figure 9. According to the tracking profiles of the three LSRMs in Figure 9a, the LSRMs are all able to follow the position reference signal. However, the control performance from the three LSRMs is not uniform. The performance of LSRM 1 is the best, and the performance of LSRM 2 is worse, that from LSRM 3 is the worst, especially as the machine approaches the peaks and valleys of the motion profile. This is because only LSRM 1 accesses the reference signal, and the response of LSRM 1 is further propagated through the communication links to LSRM 2 and further to LSRM 3. It is clear that the farther the machine is located from the reference, the worse the performance will be. In addition, there exhibits asymmetric control response during the positive and negative transitions, due to imperfect manufacture and assembly of the LSRMs.

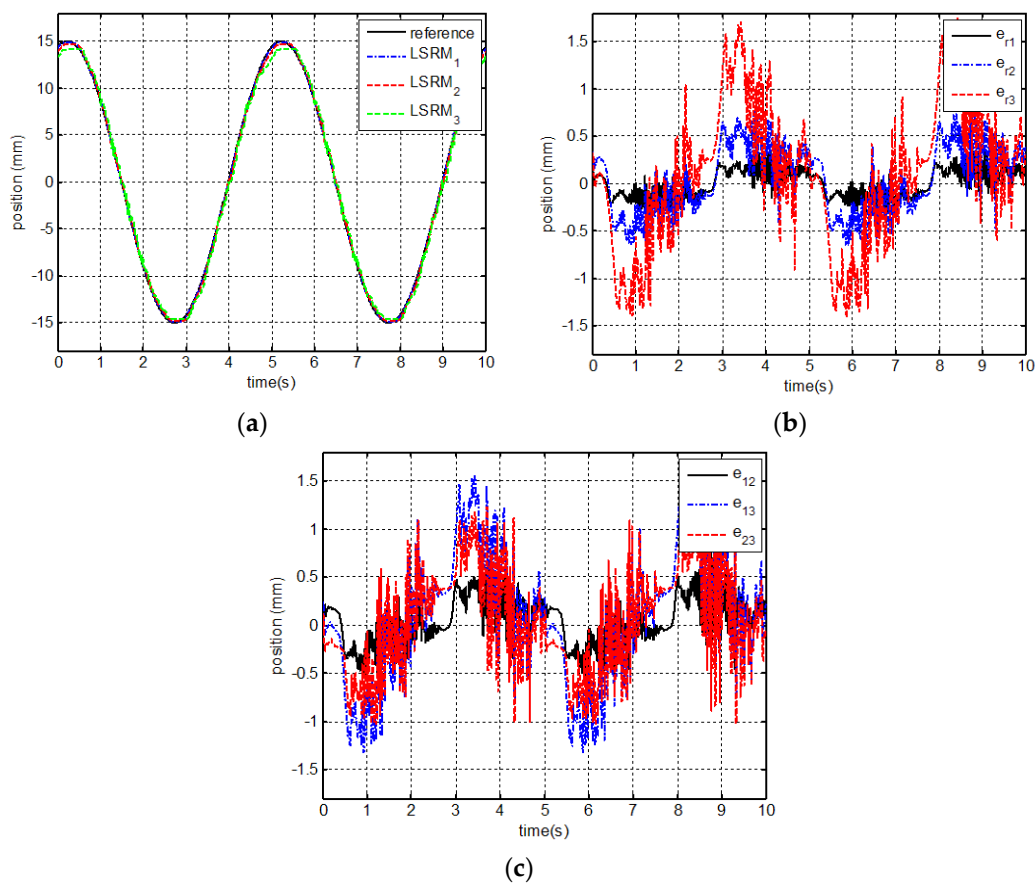


Figure 9. Tracking profiles: (a) LSRMs; (b) error to reference; and (c) relative error response with consensus algorithm only.

The error signals from the reference to the response of LSRMs can be depicted as e_{ri} ($i = 1 - 3$) and the symbol demonstrates the absolute precision of each LSRM. As shown in Figure 9b, it is clear that the relationship of error values can be depicted as $e_{r1} < e_{r2} < e_{r3}$ and the maximum positive dynamic error value exceeds 1.5 mm. The relative error from any two machines can be denoted as e_{ij} ($i, j = 1 - 3, i \neq j$), and it represents the relative precision index. It can be seen that the relative error response between LSRM 1 and LSRM 2 is better than either LSRM 1 to LSRM 3 or LSRM 2 to LSRM 3. The relationship of the relative error values can be represented as $e_{12} < e_{23} < e_{13}$, and the maximum absolute error values are approximately 1.5 mm. This is because LSRM 1 is the leader and it is directly led by the reference. Since the LSRM 2 is closest to LSRM 1, such effect is smallest, compared to that of LSRM 2 to LSRM 3 and LSRM 1 to LSRM 3.

The tracking profiles of the three LSRMs under the proposed control strategy can be found in Figure 10a. It is clear that the response waveforms are nearly uniform for either positive or negative transition according to the reference signal. Since the performance of the leader LSRM 1 is efficiently improved by the closed-loop control manner based on the feedback of the entire LSRM network, the tracking error for each LSRM to reference can be further reduced, and the maximum absolute precision falls into ± 1.3 mm, as shown in Figure 10b. From Figure 10c, the relative precision is also improved under the global feedback with the IMC strategy and the maximum dynamic error value falls into ± 1.2 mm. It can be concluded that the proposed control strategy not only improves the absolute tracking performance but also enhances the relative accuracy of all LSRMs.

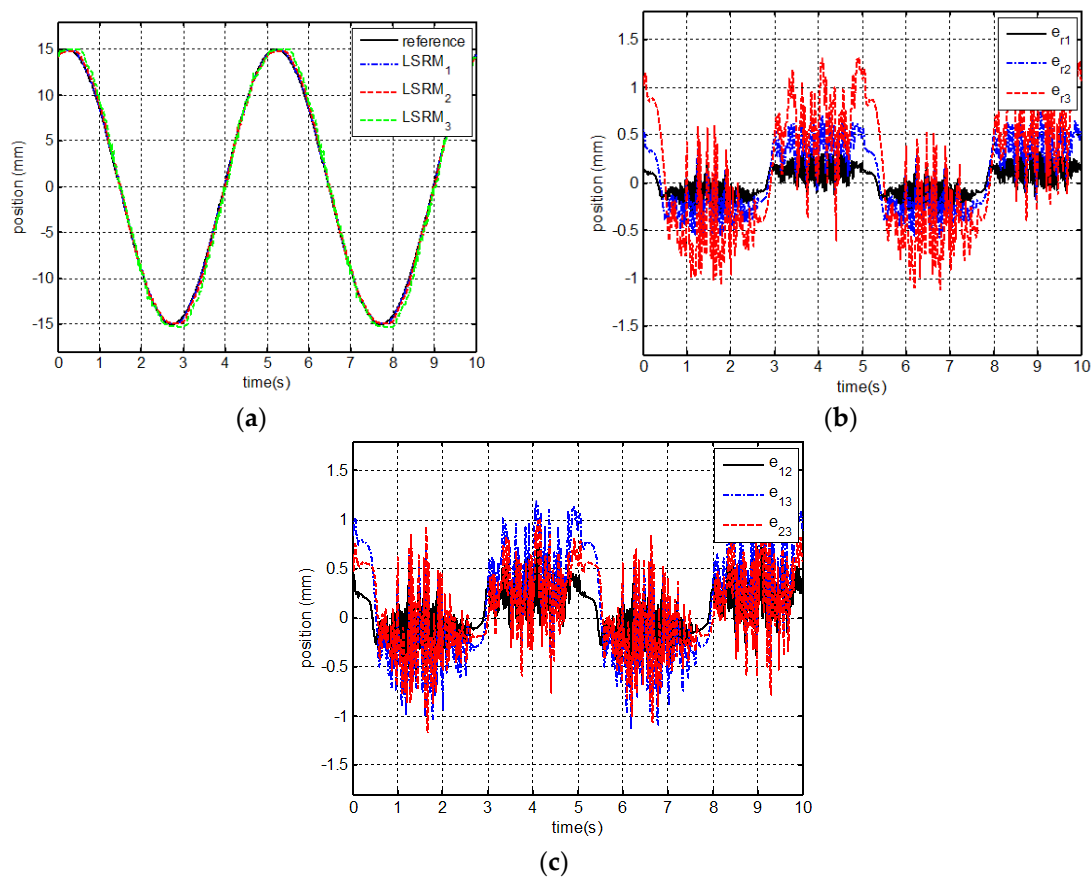


Figure 10. Tracking profiles: (a) LSRMs; (b) error to reference; and (c) relative error response under leader–follower–observer feedback with IMC.

8. Conclusions and Discussion

A leader–follower–observer network framework is proposed for a LSRM network in this paper, based on the actual requirement of a global feedback mechanism and the separation of the global controller and the observer strategy. The proposed LSRM network can be applied to the industrial field, such as in automobile frame assembly process, among other fields. The IMC is combined with the full-state feedback located on the leader, and is utilized to improve the tracking performance. The observer is responsible for the reconfiguration of the full states, and they are fed back to the leader. The conditions that guarantee the controllability and observability of the LSRM network with the IMC are also derived in this paper. Design and implementation of the global controller are performed for the LSRM network. The proposed network framework and control strategy are verified by experimentation. It can be concluded that the proposed control scheme can enhance both the absolute and the relative accuracy of the proposed leader–follower–observer LSRM network.

The previous study for the LSRM network investigates the controllability of multiple LSRMs based network and a global controller and observer is designed on one machine. This paper further investigates the technique of leader controller configuration for one machine together with the observer on the other. In addition, the communication linkage from the leader controller to the node observer is discussed, by the sparse simplification technique. Therefore, the global close loop can be realized to further improve the control performance.

Only one leader and one follower are discussed in this paper to simplify the theoretical analysis of the proposed leader–follower–observer network. Future work will concentrate on the case of multiple leaders and multiple observers, especially for the large-scale coordinated tracking

networks. More advanced control and observation algorithms can be involved to improve further the network performance.

Acknowledgments: This work was supported in part by the National Natural Science Foundation of China under Grant Nos. 51477103, 51577121, 11572248, 61690211 and 61403258. The authors also would like to thank the Guangdong and Shenzhen Governments under the Codes of S2014A030313564, 2015A010106017, 2016KZDXM007, JCYJ20160308104825040 and JCYJ20170302145012329 for support.

Author Contributions: Bo Zhang and Jianping Yuan conceived and wrote the main body of the paper. J. F. Pan designed the main body of the study. Li Qiu guided the system design, analyzed the data and revised the manuscript. Xiaoyu Wu performed the simulations and experiments. Jianjun Luo helped revise the paper.

Conflicts of Interest: The authors declare no conflict of interest.

References

1. Zhang, B.; Pan, J.F.; Yuan, J.; Rao, W.; Qiu, L.; Luo, J.; Dai, H. Tracking control with zero phase-difference for linear switched reluctance machines network. *Energies* **2017**, *10*, 949. [[CrossRef](#)]
2. Zhang, B.; Pan, J.F.; Luo, J.; Wu, X.; Qiu, L.; Pan, J.F. Hierarchical distributed motion control for multiple linear switched reluctance machines. *Energies* **2017**, *10*, 1426. [[CrossRef](#)]
3. Li, H.; Karray, F.; Basir, O.; Insop, S. A framework for coordinated control of multiagent systems and its applications. *IEEE Trans. Cybern.* **2008**, *38*, 534–548. [[CrossRef](#)]
4. Zhang, B.; Yuan, J.; Qiu, L.; Cheung, N.; Pan, J.F. Distributed coordinated motion tracking of the linear switched reluctance machine-based group control system. *IEEE Trans. Ind. Electron.* **2016**, *63*, 1480–1489. [[CrossRef](#)]
5. Sabattini, L.; Secchi, C.; Cocetti, M.; Levratti, A.; Fantuzzi, C. Implementation of coordinated complex dynamic behaviors in multirobot systems. *IEEE Trans. Robot.* **2015**, *31*, 1018–1032. [[CrossRef](#)]
6. Jia, Y.; Wang, L. Leader–follower flocking of multiple robotic fish. *IEEE/ASME Trans. Mechatron.* **2015**, *20*, 1372–1383. [[CrossRef](#)]
7. Clark, A.; Alomair, B.; Bushnell, L.; Poovendran, R. Minimizing convergence error in multi-agent systems via leader selection: A supermodular optimization Approach. *IEEE Trans. Autom. Control* **2014**, *59*, 1480–1494. [[CrossRef](#)]
8. Su, H.; Rong, Z.; Chen, M.Z.Q.; Wang, X.; Chen, G.; Wang, H. Decentralized adaptive pinning control for cluster synchronization of complex dynamical networks. *IEEE Trans. Cybern.* **2013**, *43*, 394–399. [[PubMed](#)]
9. Rosenthal, S.; Twomey, C.; Hartnett, A. Revealing the hidden networks of interaction in mobile animal groups allows prediction of complex behavioral contagion. *Proc. Natl. Acad. Sci. USA* **2015**, *112*, 4690–4695. [[CrossRef](#)] [[PubMed](#)]
10. Song, Q.; Liu, F.; Cao, J.; Yu, W. M-matrix strategies for pinning-controlled leader-following consensus in multiagent systems with nonlinear dynamics. *IEEE Trans. Cybern.* **2013**, *43*, 1688–1697. [[CrossRef](#)] [[PubMed](#)]
11. Cao, W.; Zhang, J.; Ren, W. Leader–follower consensus of linear multi-agent systems with unknown external disturbances. *Syst. Control Lett.* **2015**, *82*, 64–70. [[CrossRef](#)]
12. Chen, Y.; Shi, Y. Consensus for linear multi-agent systems with time-varying delays: A frequency domain perspective. *IEEE Trans. Cybern.* **2017**, *8*, 2143–2150. [[CrossRef](#)] [[PubMed](#)]
13. Mu, B.; Shi, Y.; Chen, J.; Chang, Y. Design and implementation of non-uniform sampling cooperative control on a group of two-wheeled mobile robots. *IEEE Trans. Ind. Electron.* **2017**, *6*, 5035–5044. [[CrossRef](#)]
14. Mu, B.; Zhang, K.; Shi, Y. Integral sliding mode flight controller design for a quadrotor and the application in a heterogeneous multi-agent system. *IEEE Trans. Ind. Electron.* **2017**, *12*, 9389–9398. [[CrossRef](#)]
15. Zeng, W.; Chow, M. Resilient distributed control in the presence of misbehaving agents in networked control systems. *IEEE Trans. Cybern.* **2014**, *44*, 2038–2049. [[CrossRef](#)] [[PubMed](#)]
16. Liu, Y.; Slotine, J.; Barabási, A. Controllability of complex networks. *Nature* **2011**, *473*, 167–173. [[CrossRef](#)] [[PubMed](#)]
17. Ruths, J.; Ruths, D. Control profiles of complex networks. *Science* **2014**, *343*, 1373–1376. [[CrossRef](#)] [[PubMed](#)]
18. Liu, Y.Y.; Slotine, J.J.; Barabási, A. Observability of complex systems. *Proc. Natl. Acad. Sci. USA* **2013**, *110*, 2460–2465. [[CrossRef](#)] [[PubMed](#)]
19. Agarwal, S.; Kachroo, P.; Contreras, S. A Dynamic Network Modeling-Based Approach for Traffic Observability Problem. *IEEE Trans. Intell. Transp. Syst.* **2016**, *17*, 1168–1178. [[CrossRef](#)]

20. Contreras, S.; Kachroo, P.; Agarwal, S. Observability and Sensor Placement Problem on Highway Segments: A Traffic Dynamics-Based Approach. *IEEE Trans. Intell. Transp. Syst.* **2016**, *17*, 848–858. [[CrossRef](#)]
21. Contreras, S.; Agarwal, S.; Kachroo, P. Quality of Traffic Observability on Highways with Lagrangian Sensors. *IEEE Trans. Autom. Sci. Eng.* **2017**, *PP*, 1–11. [[CrossRef](#)]
22. Aguilar, C.O.; Gharesifard, B. Graph controllability classes for the Laplacian leader-follower Dynamics. *IEEE Trans. Autom. Control* **2015**, *60*, 1611–1623. [[CrossRef](#)]
23. Sundaram, S.; Hadjicostis, C.N. Structural controllability and observability of linear systems over finite fields with applications to multi-agent systems. *IEEE Trans. Autom. Control* **2013**, *58*, 60–73. [[CrossRef](#)]
24. Egerstedt, M.; Martini, S.; Cao, M.; Camlibel, K.; Bicchi, A. Interacting with networks: How does structure relate to controllability in single-leader consensus networks? *IEEE Control Syst. Mag.* **2012**, *32*, 66–73. [[CrossRef](#)]
25. Zhou, T. On the controllability and observability of networked dynamic systems. *Automatica* **2015**, *52*, 63–75. [[CrossRef](#)]
26. Commault, C.; Dion, J. Input addition and leader selection for the controllability of graph-based systems. *Automatica* **2013**, *49*, 3322–3328. [[CrossRef](#)]
27. Astrom, K.J.; Murray, R.M. *Feedback Systems: An Introduction for Scientists and Engineers*; Princeton University Press: New York, NY, USA, 2008; pp. 201–220.
28. Meng, Z.; Li, Z.; Vasilakos, A.V.; Chen, S. Delay-induced synchronization of identical linear multiagent systems. *IEEE Trans. Cybern.* **2013**, *43*, 476–489. [[CrossRef](#)] [[PubMed](#)]
29. Chapman, A.; Nabi-Abdolyousefi, M.; Mesbahi, M. Controllability and observability of network-of-networks via Cartesian products. *IEEE Trans. Autom. Control* **2014**, *59*, 2668–2679. [[CrossRef](#)]
30. Pan, J.F.; Zou, Y.; Cao, G. An asymmetric linear switched reluctance motor. *IEEE Trans. Energy Convers.* **2013**, *28*, 444–451. [[CrossRef](#)]
31. Zheng, D.Z. *Linear System Theory*; Tsinghua University Publishing House: Beijing, China; Springer: Berlin, Germany, 2010; pp. 225–231.
32. Zhang, B.; Yuan, J.; Pan, J.; Wu, X.; Luo, J.; Qiu, L. Controllability and Leader-Based Feedback for Tracking the Synchronization of a Linear-Switched Reluctance Machine Network. *Energies* **2017**, *10*, 1728. [[CrossRef](#)]
33. Pan, J.F.; Zou, Y.; Cao, G. Adaptive controller for the double-sided linear switched reluctance motor based on the nonlinear inductance modeling. *IET Electr. Power Appl.* **2013**, *7*, 1–15. [[CrossRef](#)]



© 2017 by the authors. Licensee MDPI, Basel, Switzerland. This article is an open access article distributed under the terms and conditions of the Creative Commons Attribution (CC BY) license (<http://creativecommons.org/licenses/by/4.0/>).